

# Mechanical and structural analysis of graphene-PMMA laminate

Received: 28 May 2024

Accepted: 16 October 2025

Published online: 17 November 2025

Anirban Kundu<sup>1</sup>, Won Kyung Seong<sup>1</sup>✉, S. Kamal Jalali<sup>2</sup>,  
Nicola M. Pugno<sup>2,3</sup> & Rodney S. Ruoff<sup>1,4,5,6</sup>✉ARISING FROM S. Kim et al. *Nature Communications* (<https://doi.org/10.1038/s41467-024-46502-6>) (2024).

We report scientific and technical queries regarding the article reported by Kim et al.<sup>1</sup> (referred to as ref. 1 hereafter) on the mechanical properties of graphene-poly(methyl methacrylate) (PMMA) composites. The authors described a “float-stacking fabrication” method to make “graphene-PMMA laminates (GPL)” that enabled enhancing stiffness and strength well beyond PMMA alone, reporting values of tensile strength ( $\sigma$  -141 MPa) and Young’s modulus ( $E$  -5.37 GPa), with a stated graphene volume fraction of 0.19%. Our analysis finds that the reported enhancement is mainly due to the heat treatment of the polymer rather than the incorporation of graphene, and the Raman spectroscopy data further indicates large cracks and defects introduced during the hot rolling process. We believe that the queries will aid the audience in better understanding the mechanical response of graphene-PMMA composites.

## Experimental data

The thickness of each of the GPL samples (that is, all the 36 samples for GPL-0 to GPL-100) is reported as  $\sim 18 \mu\text{m}$  (17.07–19.89  $\mu\text{m}$ ), see supplementary Table 1 of ref. 1. But the SEM micrographs (Fig. 3b, c) of ref. 1 show (per our analysis of the micrographs of these 3 samples) thicknesses of  $3.66 \pm 0.10 \mu\text{m}$  (S-GPL),  $2.95 \pm 0.13 \mu\text{m}$  (T<sub>g</sub>-GPL), and  $2.35 \pm 0.13 \mu\text{m}$  (GPL) as shown in Fig. 1a. The thickness values of S-GPL and T<sub>g</sub>-GPL are not provided in ref. 1. Figure 1c and supplementary Fig. 5 of ref. 1 shows other SEM micrographs of the GPL samples. Our analysis of these SEM micrographs yields average thickness values of GPL-0 to GPL 100 as  $18.78 \pm 0.49$ ,  $21.19 \pm 0.52$ ,  $22.89 \pm 0.29$ ,  $16.40 \pm 0.35$ ,  $14.88 \pm 0.47$ , and  $18.28 \pm 0.69 \mu\text{m}$ , respectively; and  $18.14 \pm 0.54 \mu\text{m}$  from Fig. 1c. We provide the points selected for our measurements of thickness in our Fig. 1 and note that the authors of ref. 1 did not indicate where thickness measurements were made. Thickness values measured in our analysis are compared in supplementary Table 1 with the thickness values reported in ref. 1.

Enhancement in  $E$  and  $\sigma$  values of GPL-100 is compared with GPL-0 in ref. 1 to calculate the effective  $E$  and  $\sigma$  of the “graphene fillers” (as the graphene is referred to in ref. 1) present in GPL. The enhancement (in GPL-100 compared to GPL-0) in  $\sigma$  and  $E$  are reported in ref. 1 as 277.5% (from  $79.60 \pm 4.10$  to  $141.29 \pm 3.29$  MPa) and 261.26% ( $3.33 \pm 0.15$  to  $5.37 \pm 0.31$  GPa), respectively. The actual values are 77.5% (from  $79.60 \pm 4.10$  to  $141.29 \pm 3.29$  MPa) and 61.26% ( $3.33 \pm 0.15$  to  $5.37 \pm 0.31$  GPa), respectively, as per our analysis. The linear region considered for  $E$  measurements in our analysis is shown with a red dotted line in Fig. 2 (and supplementary Fig. 3) and the process is discussed in section 3 of our SI file.

The graphene PMMA stacked layers were stated to be processed with a hot rolling press to prepare the GPL. The temperature of the hot rolling press is not mentioned in ref. 1.

## Mechanical properties analysis

Ref. 1 reports  $E$  and  $\sigma$  values for graphene for sample GPL-100 of around 1.09 TPa and 33 GPa, respectively, calculated using the rule of mixtures. However, it is not clear as per ref. 1 whether these high values are for a single layer graphene<sup>2,3</sup>, or of “graphene fillers” present in the PMMA matrix.

To clearly compare the mechanical properties of graphene-PMMA laminates (GPL) with pure PMMA (GPL-0), the GPL-0 samples need to be prepared with the same number of PMMA layers as the corresponding GPL samples, using the same float-stacking method reported in ref. 1. The  $E$  and  $\sigma$  values of GPL-0 reported in ref. 1 are close to those of bulk PMMA, suggesting that GPL-0 is made of PMMA that is like regular bulk PMMA. The thickness and stress-strain curves of stacked PMMA (S-GPL-0) and stacked PMMA above the glass transition temperature (T<sub>g</sub>-GPL-0) are not reported in ref. 1. However, since their thicknesses are comparable, we assumed that their mechanical properties are like that of GPL-0.

<sup>1</sup>Center for Multidimensional Carbon Materials (CMCM), Institute for Basic Science (IBS), Ulsan, Republic of Korea. <sup>2</sup>Mechano-X Labs, Department of Civil, Environmental and Mechanical Engineering, University of Trento, Via Mesiano, Trento, Italy. <sup>3</sup>School of Engineering and Material Science, Queen Mary University of London, Mile End Road, London, UK. <sup>4</sup>Department of Chemistry, Ulsan National Institute of Science and Technology (UNIST), Ulsan, Republic of Korea. <sup>5</sup>School of Energy and Chemical Engineering, Ulsan National Institute of Science and Technology (UNIST), Ulsan, Republic of Korea. <sup>6</sup>Department of Materials Science and Engineering, Ulsan National Institute of Science and Technology (UNIST), Ulsan, Republic of Korea. ✉e-mail: [one2rang@gmail.com](mailto:one2rang@gmail.com); [ruofflab@gmail.com](mailto:ruofflab@gmail.com)

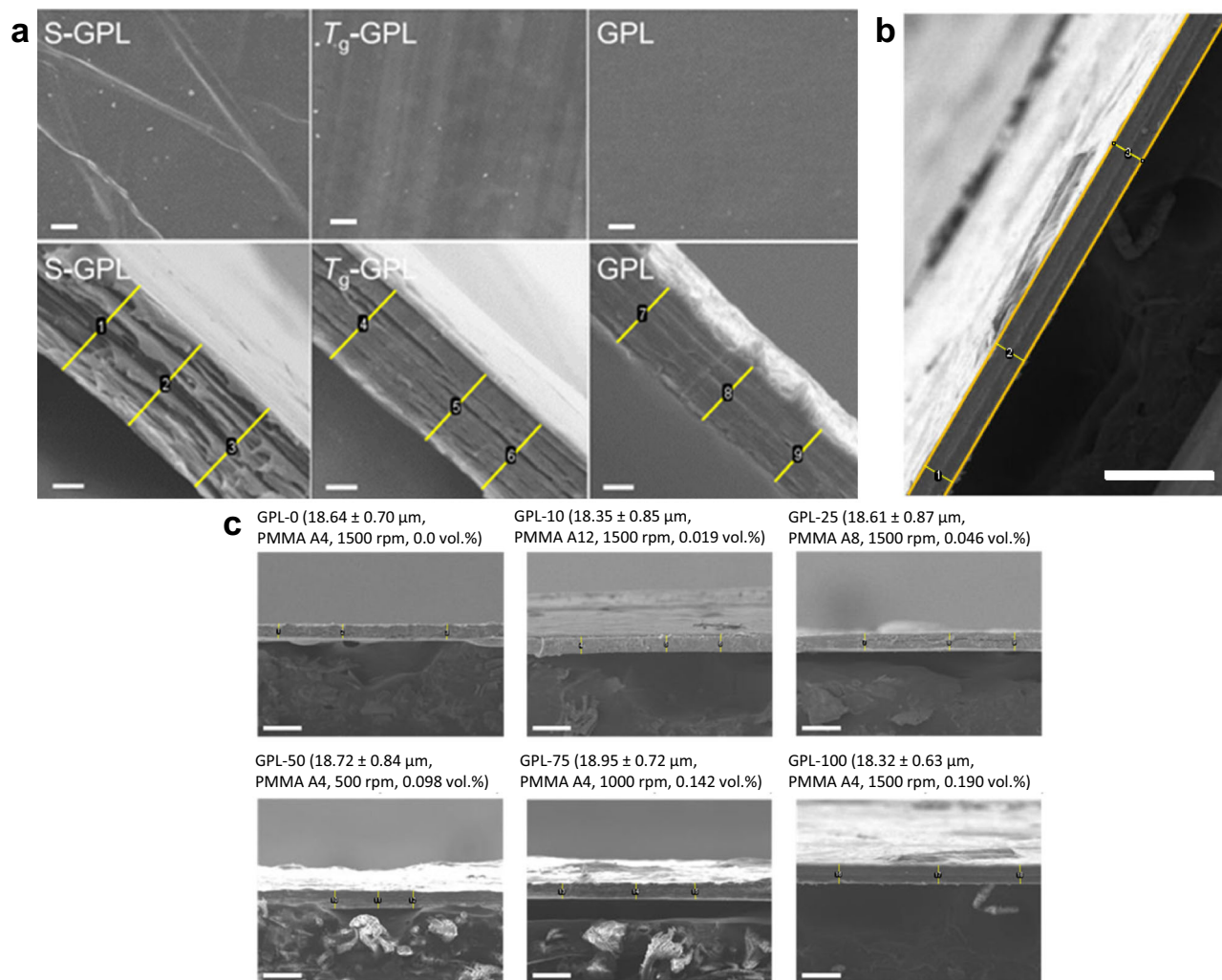


**Fig. 1 | Thickness measurements of the stacked graphene PMMA layer.** **a** The thickness of S-GPL,  $T_g$ -GPL, and GPL is found to be  $3.66 \pm 0.10$ ,  $2.95 \pm 0.13$ , and  $2.35 \pm 0.13$   $\mu\text{m}$ , respectively (image collected from Fig. 3b-c in ref. 1). **b** Thickness of GPL-100 measured from Fig. 1c (image collected from Fig. 1c of ref. 1). **c** Thickness measurement of GPL-0, GPL-10, GPL-25, GPL-50, GPL-75 and GPL-100 from supplementary Fig. 5 of ref. 1. The thickness is measured along the straight line segments (yellow) marked in the figure.

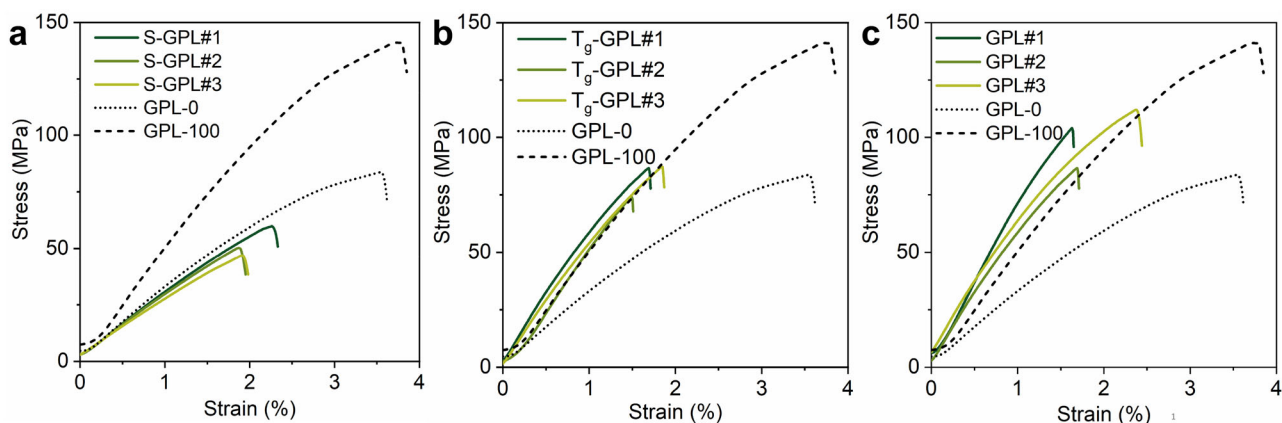


**Fig. 2 | Comparison of the stress-strain curves of the GPL samples.** Mechanical properties analysis of (a) S-GPL, (b)  $T_g$ -GPL, and (c) GPL stress strain curves compared with the stress strain curve of GPL-0 and GPL-100. The linear fitted region that is used to calculate  $E$  is discussed in Supplementary section 3. The data are drawn from the source data and supplementary Fig. 9 of ref. 1.

The stress-strain curves of three different samples (S-GPL, T<sub>g</sub>-GPL, and GPL) with 25 graphene layers are shown in supplementary Fig. 9 of ref. 1; we have analyzed these stress-strain curves (see Fig. 2) and find that our fitted  $E$  values do not match with the values shown in supplementary Table 2 of ref. 1. We summarize the  $E$  and  $\sigma$  values obtained from our Fig. 2 (note that Fig. 2 is drawn from the source data file of ref. 1) in our supplementary Table 2. The actual  $E$  for GPL (obtained by us as  $6.77 \pm 0.57$  GPa) is thus higher than GPL-100, that ref. 1 reports as the highest  $E$  ( $5.37 \pm 0.31$  GPa). It is worth noting that the average failure strain for GPL in supplementary Table 3 of ref. 1 is reported to be 1.90%, markedly differing from the GPL-100 value of 3.78% as reported in supplementary Table 2 of ref. 1. Both the GPL and GPL-100 contain the same volume fraction of graphene of 0.19% but different thicknesses. We expect they have comparable failure strains or if they are not similar, a higher failure strain for lower thickness (GPL) is expected, due to the size effect<sup>4</sup>. However, the lower thickness (GPL) exhibits a lower elongation at break (1.90%), which is unexpected.

Our analysis based on ref. 1 shows that the presence of graphene filler (25 monolayers) has a negative effect on the  $E$  and  $\sigma$  of S-GPL as compared to GPL-0. Whereas  $\sigma$  is relatively decreased for T<sub>g</sub>-GPL from GPL-0. GPL-25 shows an increase in both  $E$  and  $\sigma$  compared to GPL-0, as reported in ref. 1, with the increase in  $E$  being higher (6.77 GPa) than the reported enhancement in ref. 1 for GPL-100 (5.37 GPa). We discussed the effect of heat treatment on mechanical response of polymer in section 1 (see supplementary Fig. 1 and Fig. 2) of SI of this M-A article. As reported by Zhang et al.<sup>5</sup>, the mechanical properties of graphene are insensitive to the number of layers of graphene. However, the enhancement in  $E$  and  $\sigma$  with an increasing number of graphene layers stacked in GPL is reported in ref. 1; this seems contradictory. Ref. 1 reports that as the number of graphene layers,  $N$ , increases while maintaining a constant volume fraction, the strength of GPL initially peaks and then diminishes with further layer increments. This pattern suggests the existence of an optimal number of layers to achieve maximum strength. We have discussed this further in section 2 of Supplementary Information of this M-A article.

### Structural analysis

The reason(s) for the reported high mechanical properties of graphene in ref. 1 is/are unclear, so it is important to consider the quality of graphene used in the graphene-PMMA laminates (GPL). The mechanical properties were stated to be measured on samples with a length of 10 mm and width of 1 mm per ref. 1. However, ref. 1 only shows one TEM image of a single graphene layer embedded in the PMMA matrix, which does not provide information about the overall graphene quality/morphology in GPL at different stages of sample preparation. The SEM images ( $525 \mu\text{m} \times 440 \mu\text{m}$ ) showing the surface morphology of S-GPL, T<sub>g</sub>-GPL, and GPL (in Fig. 3b of ref. 1) also do not give information about the graphene quality (see Fig. 1a).

To understand the reinforcement effect of graphene in GPL, Raman mapping was performed on what was stated to be an 18- $\mu\text{m}$  thick sample (the thickness value mentioned in ref. 1). The Raman mapping shown over an area of  $35 \mu\text{m} \times 35 \mu\text{m}$  (supplementary Fig. 13 of ref. 1) shows no evidence of grain boundaries. The observation of grain boundaries is expected for polycrystalline graphene in Raman mapping<sup>6</sup>. Our analysis of the depth profiling data (supplementary Fig. 3 in ref. 1) suggests that it was done only at a single spot. Usually,  $I_{2D}/I_G > 2$  indicates good quality monolayer graphene, and lower values are for bilayer and multiple layers of graphene<sup>7</sup>. Our calculation shows that the depth profiling plot has an average  $I_{2D}/I_G$  of  $1.22 \pm 0.07$ ,

indicating that the graphene in GPL is not in perfect monolayer condition and is 'mixed' (in some manner) with the PMMA matrix. Our analysis of the Raman depth profiling data (in ref. 1) found that the  $I_{2D}/I_G$  value is also observed between the identified graphene layers, and this value is comparable to pristine graphene as per ref. 1. This further suggests that graphene is randomly distributed throughout the PMMA matrix, which is possible when the monolayer graphene is fragmented, perhaps due to smaller grain size and multiple grain boundaries. The hot rolling process (per ref. 1) reportedly applies a force of 78.48 N (corresponding to a compressive pressure of 8.35 MPa) to remove voids, but this removal of trapped voids seems likely to introduce large cracks and defects in graphene. It appears that the monolayer graphene present in the polymer matrix was likely fractured and fragmented during the hot rolling process, forming a graphene-PMMA composite in which the graphene is actually 'flakes' (i.e., relatively small fragments) relative to a large area CVD grown graphene.

### Conclusion

In conclusion, the float-stacking method proposed by Kim et al.<sup>1</sup> presents a promising approach for creating highly aligned graphene-polymer nanocomposites. However, there are several important issues (mentioned above) that need to be considered. It appears that the improvement in Young's modulus and strength of the stacked graphene-PMMA laminates (GPLs) reported in ref. 1 is primarily or entirely the result of temperature-induced modification of PMMA, rather than the presence of graphene. Indeed, attributing the entire improvement to the latter leads to (we suggest) grossly overestimating the properties of the polycrystalline graphene.

### Data availability

All data generated or analyzed during this study are included in this published article and its supplementary information file.

### References

1. Kim, S. I. et al. Float-stacked graphene-PMMA laminate. *Nat. Commun.* **15**, 2172 (2024).
2. Lee, G. H. et al. High-strength chemical-vapor-deposited graphene and grain boundaries. *Science* **340**, 1073–1076 (2013).
3. Qing-Yuan, L. et al. Stretch-induced stiffness enhancement of graphene grown by chemical vapor deposition. *ACS Nano* **7**, 1171–1177 (2013).
4. Abernethy, R. B. et al. *The New Weibull Handbook*. (R.B. Abernethy, 1996).
5. Zhang, Y. Y. & Gu, Y. T. Mechanical properties of graphene: effects of layer number, temperature and isotope. *Computational Mater. Sci.* **71**, 197–200 (2013).
6. Suk, J. W., Hao, Y., Liechti, K. M. & Ruoff, R. S. Impact of grain boundaries on the elastic behavior of transferred polycrystalline graphene. *Chem. Mater.* **32**, 6078–6084 (2020).
7. Wang, M. et al. Single-crystal, large-area, fold-free monolayer graphene. *Nature* **596**, 519–524 (2021).

### Acknowledgements

This work is supported by the Institute for Basic Science (IBS-R019-D1). We appreciate Daniel Hedman and Sun Hwa Lee for reading and commenting on our manuscript.

### Author contributions

All authors contributed to the analysis and interpretation of the literature that is discussed and jointly wrote the article.

## Competing interests

The authors declare no competing interests.

## Additional information

**Supplementary information** The online version contains supplementary material available at <https://doi.org/10.1038/s41467-025-66215-8>.

**Correspondence** and requests for materials should be addressed to Won Kyung Seong or Rodney S. Ruoff.

**Peer review information** *Nature Communications* thanks the anonymous reviewer(s) for their contribution to the peer review of this work.

**Reprints and permissions information** is available at <http://www.nature.com/reprints>

**Publisher's note** Springer Nature remains neutral with regard to jurisdictional claims in published maps and institutional affiliations.

**Open Access** This article is licensed under a Creative Commons Attribution-NonCommercial-NoDerivatives 4.0 International License, which permits any non-commercial use, sharing, distribution and reproduction in any medium or format, as long as you give appropriate credit to the original author(s) and the source, provide a link to the Creative Commons licence, and indicate if you modified the licensed material. You do not have permission under this licence to share adapted material derived from this article or parts of it. The images or other third party material in this article are included in the article's Creative Commons licence, unless indicated otherwise in a credit line to the material. If material is not included in the article's Creative Commons licence and your intended use is not permitted by statutory regulation or exceeds the permitted use, you will need to obtain permission directly from the copyright holder. To view a copy of this licence, visit <http://creativecommons.org/licenses/by-nc-nd/4.0/>.

© The Author(s) 2025